JOURNAL OF APPLIED ELECTROCHEMISTRY **29** (1999) 331–338.

Electrochemical deposition of zinc–polystyrene composites in the presence of surfactants

A. HOVESTAD, R. J. C. H. L. HEESEN, L. J. J. JANSSEN

Faculty of Chemical Engineering, Eindhoven University of Technology, PO Box 513, 5600 MB Eindhoven, The Netherlands

Received 11 December 1997; accepted in revised form 5 May 1998

The electrochemical codeposition of polystyrene particles and zinc on a rotating cylinder electrode was investigated. Rheological measurements indicate strong aggregation of the PS particles in the zinc deposition electrolyte. Addition of cetylpyridinium chloride, a cationic surfactant, prevents aggregation and enhances polystyrene codeposition. Other surfactants also increase suspension stability, but diminish polystyrene codeposition, irrespective of their charge. Hence, the surfactant charge does not affect polystyrene codeposition. The variation of polystyrene incorporation with the amount of suspended polystyrene, current density and electrode rotation speed signifies that polystyrene codeposition with zinc is determined by the competition between particle removal forces and particle adhesion forces at the cathode surface. The effect of the surfactants can be related to changes in surface roughness of zinc due to surfactant adsorbed on the electrode. Cetylpyridinium chloride behaves differently from the other surfactants, because it is reduced at the cathode.

Keywords: *composite plating*, *codeposition*, *polystyrene particles*, *surfactants*

List of symbols

c_i^* amount of surfactant i absorbed per unit weight of particles ($mol\,kg^{-1}$)
$\boldsymbol{F}$ force (N)
j current density ($A\,m^{-2}$)

Greek letters
α particle volume fraction in deposit
ϕ particle volume fraction in electrolyte
Γ current efficiency
$\dot{\gamma}$ shear rate (s^{-1})
τ shear stress (Pa)
ω angular velocity of rotating cylinder electrode (s^{-1})

Subscripts
a adhesion
f friction
r removal

1. Introduction

Metal matrix composite coatings, having improved properties compared to plain metal coatings, can be produced by electrochemical composite plating [1, 2]. When inert particles are suspended in a metal plating electrolyte they codeposit with the metal resulting in a dispersion of particles in a metal matrix. Usually electrochemical composite plating is used to obtain metal coatings exhibiting a specific property of the particle material: for example, a high abrasive resistance or a low coefficient of friction [1, 2]. Similarly, composites of a metal and polymer particles could replace existing metal coatings due to specific properties of the polymer material. In the present research the codeposition of Zn and polystyrene (PS) particles was investigated as a model system. Since electroplating solutions are highly concentrated electrolytes and polymer particles are hydrophobic, polymer particles are expected to aggregate in an electroplating electrolyte. Particle aggregation affects particle codeposition [3, 4] and in industrial practice it can lead to sedimentation or creaming of particles in storage tanks and clogging of tubes. Addition of a surfactant can prevent particle aggregation [3–5]. In electrochemical composite plating additional advantages are obtained when a cationic surfactant is used. The positive charge conferred on the particles by a cationic surfactant increases their attraction to the negatively charged cathode, where they codeposit [3–5]. In the present paper the effect of a cationic surfactant, namely cetylpyridinium chloride (CPC), on the codeposition of PS particles and zinc is presented. The effects of CPC is compared to that of several other surfactants.

Apart from suspension stability successful industrial application of composite plating requires operation under turbulent flow conditions and at high current densities, typically 5–10 $kA\,m^{-2}$. In the present study a rotating cylinder electrode (RCE) was

used to obtain turbulent flow conditions. The effect of rotation speed of the RCE, current density and particle electrolyte concentration on PS incorporation in Zn, both in the absence and presence of CPC, is discussed.

2. Experimental details

A $1.5\,\mathrm{kmol\,m^{-3}}$ $ZnSO_4$ $0.5\,\mathrm{kmol\,m^{-3}}$ H_3BO_3 and $0.05\,\mathrm{kmol\,m^{-3}}$ $Al_2(SO_4)_3$ solution operating at pH 3 and 318 K was the electrolyte chosen for Zn deposition, because of its anticipated use in industrial practice. PS particles with a number average diameter of $8 \times 10^{-7}\,\mathrm{m}$ were prepared by a surfactant-free emulsion polymerization [6]. Scanning electron microscope (SEM) photographs and particle size measurements show that the particles are spherical and practically monodisperse. A fresh suspension was prepared by mixing a 1.5 times concentrated solution of the electrolyte with the required amount of PS particles suspended in water. It was stirred for at least 2 h before a series of experiments, which comprised the variation of only one experimental parameter. When varying surfactant concentration surfactant was progressively added to the same suspension. After each addition the suspension was stirred for 45 min to allow the surfactant to adsorb. The surfactant concentration is expressed as the amount of moles of surfactant per kg of suspended particles

Zn–PS composites were deposited galvanostatically in a $4 \times 10^{-4}\,\mathrm{m^3}$ thermostated cylindrical glass vessel with a PVC cover. A charge of 0.8 C was applied in all experiments, which corresponds to a zinc deposit of $3 \times 10^{-5}\,\mathrm{m}$ thickness. A RCE holding interchangeable Al-cylinders with an active area of $6.7 \times 10^{-4}\,\mathrm{m^2}$ was used as cathode. Zn sheet fitted against the inner vessel wall served as anode. After degreasing and rinsing the RCE was placed in the centre of the vessel concentric with the vessel wall. In the presence of surfactant the required cell voltage was applied before the RCE was lowered into the vessel, to avoid obstruction of Zn deposition by strong surfactant adosrption onto the Al-substrate.

After deposition the substrate and deposit were rinsed, dried and weighed. Subtraction of the weight of the Al-cylinder before deposition gave the deposit weight. The PS particles were extracted from the deposit by dissolving the zinc in $4\,\mathrm{kmol\,m^{-3}}$ H_2SO4. Occasionally a few drops of $11\,\mathrm{kmol\,m^{-3}}$ H_2O_2 were needed to dissolve traces of zinc adhering to released particles. The extracted particles were recovered over a $2 \times 10^{-7}\,\mathrm{m}$ pore-size filter by vacuum filtration. After drying at 353 K for 90 min and cooling down to room temperature under vacuum, the amount of codeposited PS was obtained from the weight difference between the filter before and after filtration. Taking $1050\,\mathrm{kg\,m^{-3}}$ and $6500\,\mathrm{kg\,m^{-3}}$ for the density of the PS particles and zinc, respectively, the volume fraction included PS, α_{PS}, was calculated.

A few composite deposits were studied using a Cambridge Stereoscan S200 scanning electron microscope (SEM) before composition analysis. Additionally, composites prepared in a $2.5 \times 10^{-3}\,\mathrm{m^3}$ Hull cell were investigated. The trapezoidal shape of a Hull cell allows simultaneous deposition at a range of current densities. A magnetic strirrer was used to keep the particles suspended. The composite deposit was thoroughly rinsed with water and acetone and dried. A thin Au coating was sputtered onto samples cut from the Hull cell deposits to enable the observation of the nonconducting PS-particles.

3. Results

3.1. *Suspension stability*

Aggregation of particles in dilute suspensions ($\phi < 0.3$) is demonstrated by deviations from Newtonian viscous behaviour [7, 8]. Rheological measurements in suspensions of various PS volume fractions, both in the absence and presence of CPC, were performed using a concentric cylinder type viscometer (Brookfield DV II) [9]. Figure 1 shows the shear stress, τ, against the shear rate $\dot{\gamma}$, at various volume fraction ϕ at 298 K. In surfactant-free suspensions thixotropy was observed. These suspensions show Bingham-type viscous behaviour, signifying strong aggregation of the PS particles. A pseudo yield stress required to break up long range particle structures and to obtain continuous shearing is found [8].

Microscopical examination of suspensions with $\phi_{PS} = 0.004$, confirms the presence of large aggregates in the absence of surfactant [9]. Addition of $0.3\,\mathrm{mol\ CPC\,kg^{-1}}$ of PS particles does not yield a suspension without aggregates, although their size is strongly reduced. However, these suspensions do exhibit Newtonian viscous behaviour (Figure 1). It can be concluded that CPC does not prevent PS particle aggregation, but that a small shear is sufficient to break up the aggregates into single particles. The same is found on addition of $0.3\,\mathrm{mol\,kg^{-1}}$ of

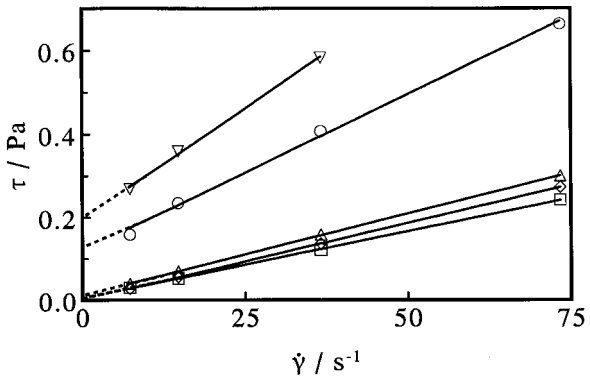

Fig. 1. Shear stress as a function of the applied shear rate for various amounts of PS particles suspended in Zn deposition electrolyte at 298 K, ϕ_{PS}: 0 (◇); 0.01 (△); 0.05 (◯); 0.08 (▽); 0.05 + $0.2\,\mathrm{mol\,kg^{-1}}$ CPC (□). Lines represent linear fits.

other cationic surfactants, cetytrimetylammonium bromide (CTAB) and cetyltrimetylammonium chloride (CTAC). In the presence of the anionic surfactant, sodium dodecylsulphate (SDS) no aggregates are observed, whereas the non-ionic surfactant, nonylphenol (ethoxylate)$_{28}$(propoxylate)$_{13}$(NPE1800), does not prevent aggregation.

3.2. *Surfactant type and concentration*

When investigating the effect of surfactant concentration on codeposition the adsorption of the surfactant on the particles has to be considered. Only adsorbed surfactant contributes to the particle–cathode interaction. Moreover, free surfactant, that is surfactant not adsorbed on particles, adsorbs on the cathode, which may affect deposit properties. The optimal surfactant concentration for codeposition is the concentration, where the adsorption of the surfactant on the particles is maximal [3, 5]. Using the soap titration method developed by Maron *et al.* [10–12], a maximum amount of 0.02 mol CPC adsorbed per kg of PS particles was determined [9]. For all volume fractions PS of interest, that is $\phi_{PS} > 0.001$, the free surfactant concentration is negligible compared to the total concentration of added surfactant. Consequently, it can be concluded that to obtain maximum CPC adsorption a total amount of $c^* = 0.02$ mol CPC kg^{-1} of PS particles has to be added. From [13–15] it may be deduced that c^* for CTAB, CTAC and SDS will be close to that of CPC, while for NPE1800 it will be a factor of 2 to 5 lower [16].

The amount of PS codepositing from suspensions with $\phi_{PS} = 0.02$ was determined as a function of concentration of the various surfactants. The results are shown in Fig. 2 for CPC, SDS and NPE1800 and in Figure 3 for CPC, CTAB and CTAC. At surfactant concentrations lower than 0.005 mol kg^{-1} the volume fraction of codeposited PS is equal to that without surfactant, namely 0.06 ± 0.02, independent of surfactant type and concentration. In the presence of CPC codeposition remains constant up to the concentration at maximum adsorption. At higher CPC concentrations a strong increase, up to a factor of 3, in PS codeposition with c^*_{CPC} is found. Besides, the deposit quality is strongly reduced at these high CPC concentrations (Section 3.5). At higher SDS or NPE1800 concentration codeposition is reduced and for $c^* > 0.01$ mol kg^{-1} no significant codeposition can be detected. A similar trend is found for CTAB and CTAC although the decrease in codeposition is less dramatic and occurs at slightly higher concentrations.

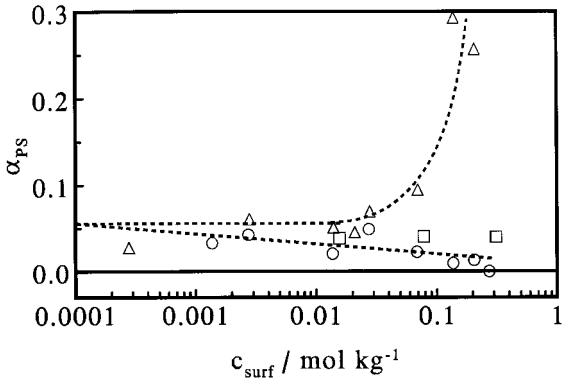

Fig. 3. Volume fraction of codeposited PS particles against the concentration of three cationic surfactants at $j = 0.5$ kA m^{-2}, $\omega = 100$ s^{-1} and $\phi_{PS} = 0.02$; CPC (△); CTAB (○) and CTAC (□).

3.3. *Particle concentration*

In Fig. 4 the effect of the amount of suspended PS particles on their codeposition with Zn is given at three different CPC concentrations. In accordance with Figs 2 and 3 practically no difference in codeposition is found between a CPC-free suspension and one containing 0.02 mol kg^{-1} CPC. In the presence of 0.2 mol kg^{-1} CPC considerably higher codeposition is obtained. At all three CPC concentrations an increase in codeposition with the amount of suspended particles is found. As generally observed [1, 2] the vari-

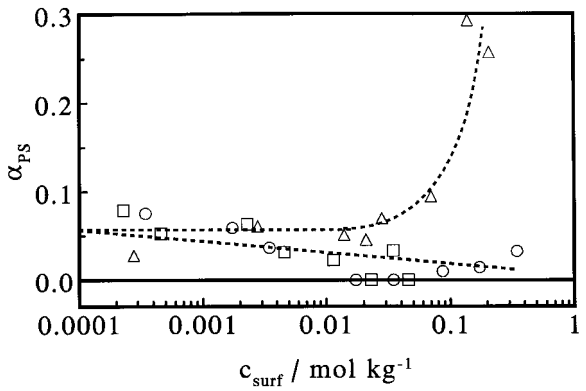

Fig. 2. Volume fraction of codeposited PS particles against the concentration of various surfactants at $j = 0.5$ kA m^{-2}, $\omega = 100$ s^{-1} and $\phi_{PS} = 0.02$; CPC (△); SDS (○) and NPE1800 (□).

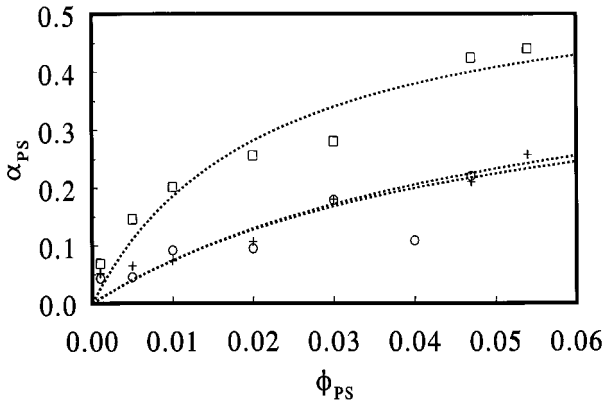

Fig. 4. Volume fraction of codeposited PS particles against the volume fraction of suspended particles at several concentrations of CPC at $j = 0.5$ kA m^{-2}, $\omega = 100$ s^{-1} and c^*_{CPC} is 0 (○); 0.02 mol kg^{-1} (+) and 0.2 mol kg^{-1} (□). Dotted lines are fits with a Langmuir isotherm.

ation of α_{PS} with ϕ_{PS} can be described by a Langmuir-type adsorption isotherm (dotted lines in Fig. 4). In the presence of 0.2 mol kg^{-1} CPC the α_{PS} at $\phi_{PS} > 0.035$ are higher than expected from the behaviour at low ϕ_{PS}.

3.4. *Current density*

The variation in PS codeposition with current density is shown in Fig. 5 with and without CPC addition. In all cases PS codeposition is practically unaffected by the current density from $j = 0.5$ to 7.5 kA m^{-2}. It can be concluded that considerable PS codeposition is obtained at current densities suitable for industrial application. For $c^*_{CPC} = 0$ and 0.02 mol kg^{-1} a peak in the curve of α_{PS} against current density is observed at 0.05 and 0.2 kA m^{-2}, respectively. Similar peaks have been reported for various codeposition systems [1, 2]. In the presence of 0.2 mol kg^{-1} CPC for $j < 0.5$ kA m^{-2} on certain parts of the electrodes Zn deposition was inhibited by the deposition of an organic material.

From the weight of deposited zinc and the applied current density the current efficiency for zinc deposition, Γ, was calculated using Faraday's law. For all experimental conditions it was found that $0.90 < \Gamma < 1$. Taking into account the experimental accuracy this is close to the value of 1 generally reported for zinc deposition [17, 18]. Even on addition of surfactants no significant change in zinc deposition current efficiency was observed.

3.5. *Electrode rotation speed*

Since at a rotation speed, ω, larger than 6 s^{-1} the RCE operates in the turbulent flow regime [19], it can be concluded from the foregoing results that PS particles codeposit appreciably under turbulent flow conditions. The effect of the electrode rotation speed on PS codeposition at $j = 0.5$ kA m^{-2} is presented in Fig. 6. PS codeposition in the presence of 0.2 mol kg^{-1} CPC does not vary with rotation speed up to $\omega = 225$ s^{-1} and decreases with ω at higher rotation speeds. On the other hand the amount of

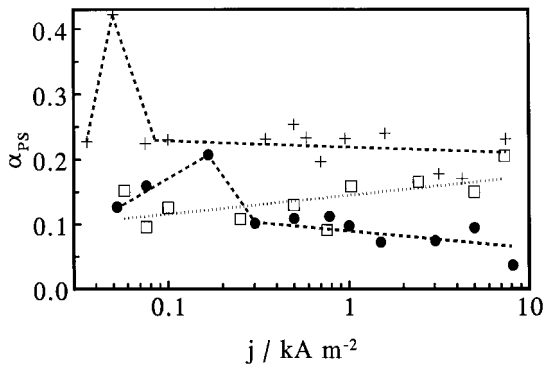

Fig. 5. Volume fraction of codeposited PS particles against current density at $\omega = 100$ s^{-1}, $\phi_{PS} = 0.02$ and $c^*_{CPC} = 0$ (●); $\phi_{PS} = 0.054$ and $c^*_{CPC} = 0.02$ mol kg^{-1} (+); $\phi_{PS} = 0.02$ and $c^*_{CPC} = 0.2$ mol kg^{-1} (□).

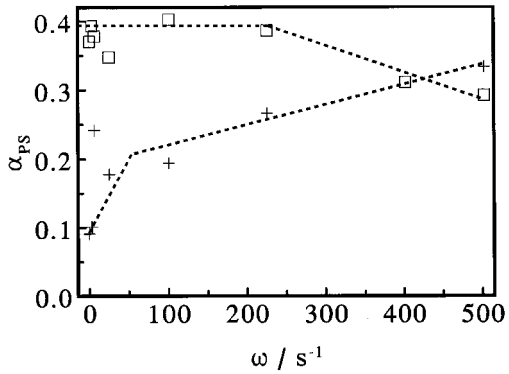

Fig. 6. Volume fraction of codeposited PS particles against the electrode rotation speed at $j = 0.5$ kA m^{-2}, $\phi_{PS} = 0.054$ and $c^*_{CPC} = 0.02$ mol kg^{-1} (+); $\phi_{PS} = 0.02$ and $c^*_{CPC} = 0.2$ mol kg^{-1} (□).

codeposited PS rises almost continuously with ω in the presence of 0.02 mol kg^{-1} CPC. At very low rotation speeds, that is $\omega < 25$ s^{-1}, the RCE is not able to keep the aggregated particles suspended. This results in a depletion of particles from the bulk of the suspension and lower codeposition.

In the absence of surfactant creaming of the electrolyte suspension at high rotation speeds was observed. On top of the suspension a layer of particle foam was formed, which could hardly be resuspended. Codeposition from a suspension with $\phi_{PS} = 0.04$ increased continuously in successive experiments, despite the fact that the rotation speed was varied randomly. Moreover, the volume fraction codeposited PS at $\omega = 100$ s^{-1} was three times as high at the end of a series of experiments as at the start. This behaviour is a consequence of the thixotropy found during rheological measurements. The duration of an experiment is of the same order as the time required to reach a steady state between aggregate break up and formation after a change in shear rate. Therefore, measurements at alternately high and low rotation speed, $\omega = 400$ and 25 s^{-1}, respectively, were performed in a $\phi_{PS} = 0.02$ suspension. After four experiments a steady state was reached, where codeposition at both rotation speeds was constant. It was found that codeposition was highest at $\omega = 400$ s^{-1}.

3.6. *Surface appearance and morphology*

SEM photomicrographs of the surface of composites prepared in the Hull cell or the RCE are presented in Figs 7–10. Zinc deposited from a particle-free electrolyte appears dull light grey. Stacks of hexagonal platelets orientated at random angles to the substrate, characteristic for zinc deposited from acidic $ZnSO_4$ electrolytes [20, 21] are observed [9]. At $j = 500$ A m^{-2} suspension containing 0 to 0.02 mol kg^{-1} CPC yielded a morphology comparable to that obtained from a particle-free electrolyte (Fig. 7).

At lower current density, $j = 50$ A m^{-2}, a so-called mossy zinc deposit was obtained (Fig. 8). Mossy de-

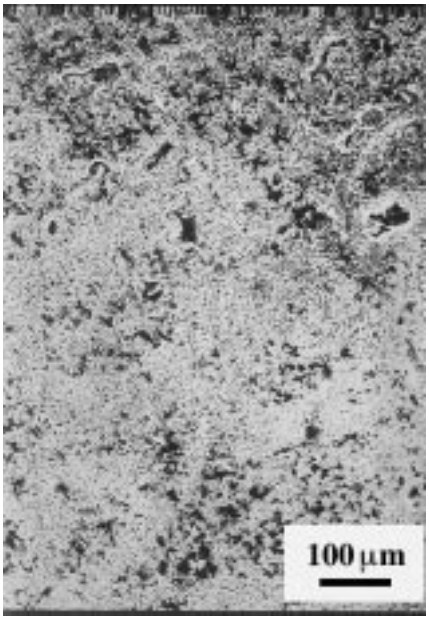

Fig. 7. SEM photomicrograph of composite surface morphology; $\phi_{PS} = 0.047$, $\omega = 100\,s^{-1}$ and $c^*_{CPC} = 0.02\,mol\,kg^{-1}$; $j = 500\,A\,m^{-2}$.

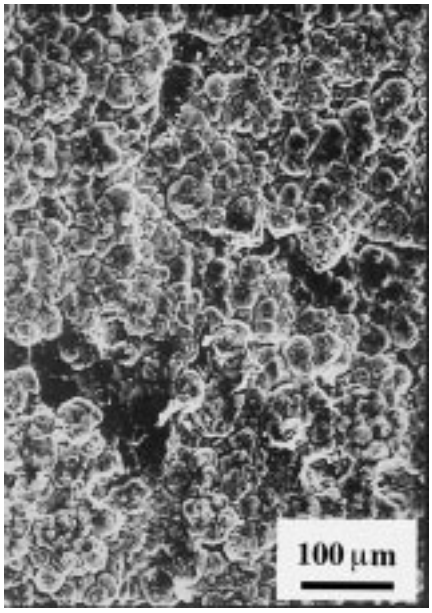

Fig. 9. SEM photomicrograph of composite surface morphology; $\phi_{PS} = 0.054$, $c^*_{CPC} = 0.2\,mol\,kg^{-1}$; $j = 500\,A\,m^{-2}$ $\omega = 100\,s^{-1}$.

posits consists of spongy nodules made up of very small zinc crystallites and are characteristic for zinc deposited at low current densities [17, 22]. In between the nodules PS particle agglomerates were present. Under these conditions PS particles codeposition was high (Fig. 6). Similarly, in the presence of $0.2\,mol\,kg^{-1}$ CPC and $\phi_{PS} = 0.047$ PS incorporation was high and a nodular deposit was formed (Fig. 9). The nodules were $(1–10) \times 10^{-5}\,m$ in diameter and in between the nodules areas covered with the organic material mentioned in Section 3.3 were present. The deposit quality was poor; the composites were black and brittle.

Addition of $0.3\,mol\,kg^{-1}$ CTAC to a $\phi_{PS} = 0.02$ suspension yielded a network of needle-like crystallites with a diameter smaller than $1 \times 10^{-6}\,m$ (Fig. 10). The deposit was smooth and slightly shiny, but darker than in the absence of surfactant. The changes in appearance on addition of CTAB, SDS and NPE1800 were similar to that on CTAC addition. At these high surfactant concentrations PS codeposition was negligible for all these surfactants.

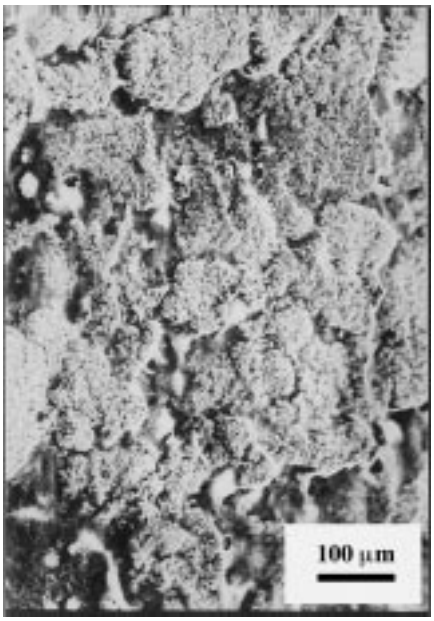

Fig. 8. SEM photomicrograph of composite surface morphology; $\phi_{PS} = 0.054$, $\omega = 100\,s^{-1}$ and $c^*_{CPC} = 0.02\,mol\,kg^{-1}$; $j = 50\,A\,m^{-2}$.

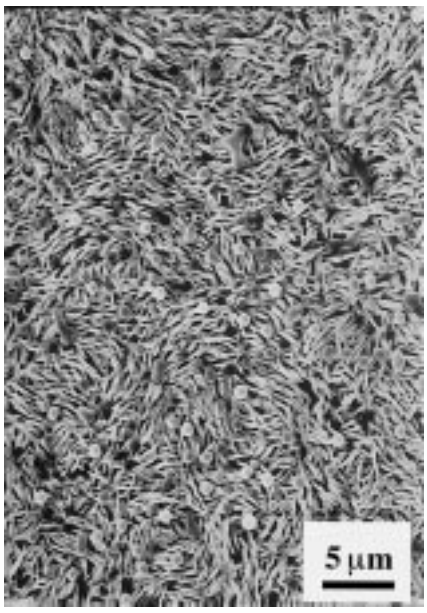

Fig. 10. SEM photomicrograph of composite surface morphology; $\phi_{PS} = 0.02$, $c^*_{CTAC} = 0.3\,mol\,kg^{-1}$; and $500 < j < 900\,A\,m^{-2}$ (Hull cell).

4. Discussion

4.1. *Particle incorporation mechanism*

The mechanism underlying electrochemical codeposition of particles and a metal can be generalized to a two step-process: namely, transfer of the particles from the bulk to the electrode surface followed by a particle–electrode interaction leading to particle incorporation [23, 24]. The practically constant codeposition over a wide range of current densities implies that the particle–electrode interaction is rate-determining in PS codeposition with zinc. In the presence of $0.2\,\mathrm{mol\,kg^{-1}}$ CPC this is supported by the negligible effect of the electrode rotation speed on codeposition. The exact nature of the particle–electrode has still to be elucidated. In the mechanism proposed by Fransaer [23, 24] the particle–electrode interaction is described by a force balance on a particle at the electrode surface (Fig. 11). Forces tending to remove particles from the electrode, $\boldsymbol{F}_r$, are counteracted by a friction force. $\boldsymbol{F}_f$, which results from forces responsible for particle adhesion, $\boldsymbol{F}_a$. The adhesion forces consists of particle–electrode interaction forces, like the London–van der Waals force, the electroosmotic force, the electrophoretic force and the hydration force. Depending on the electrode geometry forces acting only on the particles, like gravity, buoyancy and hydrodynamic forces, contribute to $\boldsymbol{F}_a$. The removal forces, $\boldsymbol{F}_r$, are of hydrodynamical origin, for example due to electrode rotation.

4.2. *Adhesion forces*

4.2.1. Electroosmotic and electrophoretic force. The electroosmotic and electrophoretic force are a result of the surface charge of the particles and electrode, which brings about an electrical double layer. The electroosmotic force arises when the electrical double layers of a particle and the electrode overlap. The electrophoretic force is due to the action of the applied electrical field on the particle double layer. Adsorption of ionic surfactants on particles is therefore believed to affect particle codeposition [3–5]. It is obvious that this effect becomes increasingly important with increasing amount of surfactant adsorbed on the particles. However, no significant change in codeposition with any of the surfactants at concentrations lower than the concentration at maximum adsorption was observed.

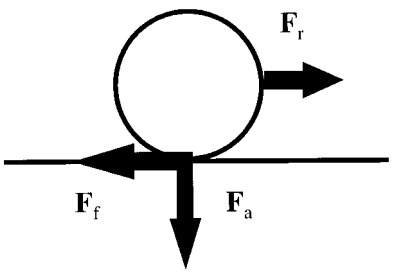

Fig. 11. Force balance on a particle adsorbed on the electrode; $\boldsymbol{F}_f$ is the friction force, $\boldsymbol{F}_a$ is the adhesion force and $\boldsymbol{F}_r$ is the removal force [23, 24].

The electroosmotic force also acts between particles and opposes particle aggregation. The aggregation of PS particles in the electrolyte, even in the presence of $0.3\,\mathrm{mol\,kg^{-1}}$ surfactant, shows that the electroosmotic between particles is negligible in the zinc deposition electrolyte. At higher concentrations the surfactants do affect PS codeposition. Additional adsorption of cationic surfactants on PS particles has been observed in electrolytes, but the extent of the extra adsorption is too small to explain the observations [15]. It can be concluded that the electroosmotic and electrophoretic force do not affect PS codeposition. The electrical double layers of the particles and the electrode are strongly compressed due to the high electrolyte concentration, even in the presence of adsorbed surfactants.

4.2.2. Hydration force. At the concentrations were surfactants affect PS codeposition surfactant adsorption on the growing zinc layer becomes significant as exemplified by the changes in the appearance and morphology of the composites. Surfactant adsorption on the electrode differs from adsorption on the particles, because the electrode surface is continuously renewed during metal deposition. Electrochemical investigations on the adsorption of CTAB and CPC on mercury show that CPC is electrochemical reducible at potentials more negative than −0.71 V vs SHE [25–27]. CPC reduces to a dimeric species, which remains adsorbed onto the electrode [26, 27]. Since the equilibrium potential of the Zn^{2+}/Zn couple is −0.76 V vs SHE [28], reduction of CPC, absorbed on the cathode, can occur during zinc deposition. This may explain the organic material observed on the electrodes in the presence of large amounts of CPC.

Fransaer *et al.* [23, 24] proposed the hydration or structural force as the adhesion force governing particle incorporation. This repulsive force arises from the work required to remove the ordered hydration layers at the solid–liquid interfaces of solids coming into close contact [29, 30]. Hence, it can be argued that the hydrophobic nature of the adsorbed CPC dimer diminishes the hydration force and enhances PS codeposition. In contrast a strong repulsive hydration force between the surfactant layers on the electrode and a approaching particle decreases PS codeposition in the presence of the other surfactants. For CTAB adsorbed on mica surfaces in a $1.5\,\mathrm{mol\,m^{-3}}$ NaCl electrolyte a short-range repulsive force ascribed to hydration effects has been measured [29].

In [23, 24] it is suggested that the changes in hydrophobicity of the particles due to surfactant adsorption determine the effect of surfactants on particle codeposition. However, up to the concentration at maximum adsorption surfactants hardly affect PS codeposition, although the particles become

increasingly hydrophilic. Moreover, the peak in a particle incorporation against current density curve is attributed a minimum in the hydration force at the potential of zero charge (p.z.c.) of the depositing metal [23, 24]. This would require the p.z.c. of Zn in the zinc deposition electrolyte to be shifted about 0.2 V in the cathodic direction with respect to its p.z.c. in 1 kmol m^{-3} $NaSO_4$ [28]. Thus a description of zinc polystyrene codeposition using the hydration force is not very satisfactory.

4.2.3. Other adhesion forces. Excluding the electro-osmotic, electrophoretic and the hydration force, the London–van der Waals force remains as the main force responsible for PS particle adhesion to the electrode. Because this force cannot explain the effect of surfactants on PS codeposition with zinc the other forces, that is $\boldsymbol{F}_r$ and $\boldsymbol{F}_f$, have to be considered.

4.3. *Friction force*

The friction force, which prevents a particle from being removed from the surface before being incorporated depends on the local surface roughness around the particle. A particle adsorbed in a recessed area has a much larger probability of becoming included than one adsorbed on a flat surface. Particularly if particles are able to move along the surface to recessed areas due to shearing forces or Brownian rotation, a rough surface will lead to a higher amount of incorporated particles. It was observed that changes in deposit appearance and surface morphology correlate with changes in PS codeposition. Therefore it is proposed that a change in surface roughness, due to the change in the free surfactant concentration, is responsible for the differences in PS codeposition.

Figure 12 shows a generalized picture of the main types of growth morphologies, which can be encountered for zinc deposition [20, 21]. Particles are depicted in the figure to show how they can be adsorbed onto the deposit. A basal type of deposit is obtained in the presence of impurities, like Co, Ni and Sb, which deposit in between the stacks of platelets resulting in a nodular structure [20, 21 ,31, 32]. Figure 9 shows such a morphology in the presence of high CPC concentrations, where the dimeric product of CPC reduction has deposited in between the nodules. Addition of organics changes the morphology to the vertical type [20, 21, 31, 32]. Comparison of Fig. 10 with Fig. 12 shows that CTAC has a similar effect on the composite deposits. Up to $c_i^* = 0.02\,\text{mol}\,\text{kg}^{-1}$ the intermediate type of growth is observed (Fig. 7). Comparing the roughness associated with the growth morphologies of zinc, particle incorporation will decrease in the order: basal, intermediate and vertical type. Correspondingly, PS codeposition is the largest at high concentrations of CPC, the lowest with high concentrations of CTAC or the other surfactants and in between for suspensions containing up to 0.02 mol kg^{-1} surfactant.

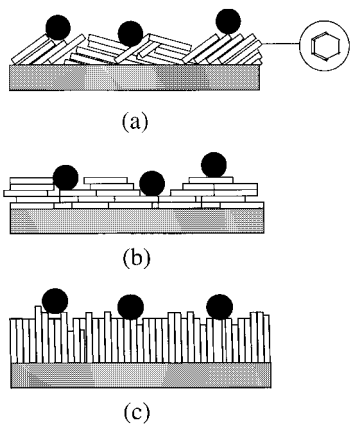

Fig. 12. Growth morphologies of zinc deposits; (a) intermediate type, (b) basal type, (c) vertical type [20]. Black spots represent particles.

A similar reasoning can explain the peaks at low current density in the α_{PS} against j curves (Fig. 5). A deposit consisting of mossy nodules was found at the peak in the presence of 0.02 mol kg^{-1} CPC (Fig. 8). Similar to composites prepared at high CPC concentrations this is a basal type of morphology, where increased codeposition compared to the intermediate type of morphology obtained at higher current densities is expected. It has often been observed that the peaks in particle incorporation occur at the same current density as kinks in the polarisation curve for metal deposition [23, 24, 33–35]. The peaks in PS codeposition appear around the current density, where Wiart *et al.* [17,18] found an 'S'-type kink in galvanostatic polarization curves for Zn deposition from an acidic $ZnSO_4$ electrolyte. Here the morphology changes from the mossy basal type to the compact intermediate type.

4.4. *Removal force*

The changes in α_{PS} with ω affirm that hydrodynamics also have to be considered. The electrode rotation exerts a removal force ($\boldsymbol{F}_r$) on particles at the electrode surface. If this force becomes larger than the friction force, particles are removed from the electrode surface [23, 24] Due to surface heterogeneity, like the surface roughness, this condition will not be reached by all adsorbed particles at the same electrode rotation speed [23, 24]. At high rotation speeds the rate of PS particle removal becomes larger than that of attachment at certain sites on the electrode. As a result PS codeposition in the presence of 0.2 mol kg^{-1} CPC is reduced at $\omega > 225\,s^{-1}$ (Fig. 6). In aggregated suspensions, that is without surfactant or with 0.02 mol kg^{-1} CPC, the effect of hydrodynamics on PS codeposition is more complex. The change in removal force with electrode rotation speed is different, because the viscosity of the suspension decreases with shear rate (Fig. 1). Apart from aggregate removal, changes in aggregate size with shear rate play a role [36]. Consequently, an explanation

for the increase in α_{PS} with ω in aggregated suspensions cannot easily be given.

Also the enhanced codeposition at $\phi_{PS} > 0.035$ when $c^*_{CPC} = 0.2\,\mathrm{mol\,kg^{-1}}$ compared to the extrapolated Langmuir behaviour at lower ϕ_{PS} could be due to hydrodynamic effects. A similar increase in PS codeposition with Cu at higher amounts of suspended particles is explained by hydrodynamic interactions of suspended particles with other either suspended or adsorbed particles [23, 24]. In adsorption theory additional adsorption at higher adsorbate concentration is usually attributed to a second adsorption process [37]. At $\phi_{PS} > 0.035$ PS particles could adsorb on top of particles already adsorbed at the electrode surface or onto less active electrode surface sites.

5. Conclusions

It has been shown that polystyrene particles codeposit with zinc in volume fractions as large as 0.4 under turbulent flow conditions. Up to current densities of $8\,\mathrm{kA\,m^{-2}}$ composites containing an appreciable amount of PS particles can be obtained. The effect of the experimental parameters on PS codeposition with zinc can be explained using the mechanism proposed by Fransaer *et al.* [23, 24], that is the competition between particle adhesion and particle removal forces at the electrode surface.

By contrast with expectation, cationic surfactants do not have a beneficial effect on PS codeposition. In fact, with the exception of CPC, all types of surfactant strongly diminish codeposition at high concentrations. CPC does enhance codeposition, but this is related to its reduction at the cathode and subsequent deposition on the growing zinc layer. Unfortunately, the deposit quality is strongly reduced in the presence of CPC. It is proposed that differences in particle removal due to differences in surface roughness are responsible for the effect of surfactants on PS codeposition.

Acknowledgement

The authors would like to acknowledge the Packaging Technology Department of the Corporate Research Laboratory of Hoogovens Groep BV, IJmuiden for financially supporting this research.

References

[1] J. R. Roos, J. P. Celis, J. Fransaer and C. Buelens, *J. Metals* **42** (1990) 60.
[2] A. Hovestad and L. J. J. Janssen, *J. Appl. Electrochem.* **25** (1995) 519.
[3] K. Helle, Report AKZO Research, Arnhem (1993).
[4] K. Helle, Proceedings, 4th International Conference on 'Organic Coating Science and Technology', Athens (1978), p. 264.
[5] P. K. N. Bartlett, Industrial training report AKZO, Arnhem (1980), pp. 10–39.
[6] G. Tuin, A. C. I. A. Peters, A. J. G. van Diemen and H. N. Stein, *J. Colloid Interface Sci.* **158** (1993) 508.
[7] J. Laven, F. J. Huisman, L. J. Lalieu and H. N. Stein, *Colloids and Surfaces* **31** (1988) 385.
[8] H. A. Barnes, J. F. Hutton and K. Walters, 'An Introduction to Rheology' (Elsevier Science, Amsterdam, 1989), pp. 115–39.
[9] A. Hovestad, PhD thesis, Eindhoven University of Technology (1997).
[10] S. H. Maron, M. E. Elder and M. E. Ulevitch, *J. Colloid Interface Sci.* **9** (1954) 89.
[11] S. H. Maron, M. E. Elder and M. E. Ulevitch, *J. Colloid Interface Sci.* **9** (1954) 104.
[12] K. J. Abbey, J. R. Erickson, R. J. Seidewand, *J. Colloid Interface Sci.* **66** (1978) 203.
[13] P. Conner, R. H. Ottewill, S., *J. Colloid Interface Sci.* **37** (1971) 642.
[14] G. Tuin and H. N. Stein, *Langmuir* **10** (1994) 1054.
[15] J. Zhao and W. Brown, *Langmuir* **11** (1995) 2944.
[16] A. van den Boomgaard, PhD thesis, Agriculture University of Wageningen (1985).
[17] J. Bressan and R. Wiart, *J. Appl. Electrochem.* **9** (1979) 43.
[18] I. Epelboin, M. Ksouri and R. Wiart, *J. Electrochem. Soc.* **122** (1975) 1206.
[19] D. R. Gabe, *J. Appl. Electrochem.* **13** (1983) 3.
[20] R. C. Kerby, *in* 'Application of Polarization Measurements in the Control of Metal Deposition', Process Metallurgy 3, edited by I. H. Warren (Elsevier Science, Amsterdam, 1984), p. 111.
[21] D. J. MacKinnon, J. M. Brannen and P. L. Fenn, *J. Appl. Electrochem.* **17** (1987) 1129.
[22] J. N. Jovićević, D. M. Drażić and A. R. Despić, *Electrochim. Acta* **22** (1977) 589.
[23] J. Fransaer, J. P. Celis and J. R. Roos, *J. Electrochem. Soc.* **139** (1992) 413.
[24] J. Fransaer, PhD thesis, Catholic University of Leuven (1994).
[25] A. Pappa-Lousi, P. Nikitas and Ph. Andonoglou, *Electrochim. Acta* **39** (1994) 375.
[26] P. Nikitas, A. Paapa-Louisi and S. Antoniou, *J. Eletroanal. Chem.* **367** (1994) 239.
[27] L. N. Nekrasov, H. Almualla, T. N. Khomchenko, Yu. D. Smirnov and A. P. Tomilov, *Russ. J. Electrochem.* **30** (1994) 73.
[28] A. J. Bard, 'Encyclopedia of Electrochemistry of the Elements', Vol. 5 (Marcel Dekker, New York, 1982), p. 1.
[29] R. M. Pashley and J. N. Israelachvili, *J. Colloid Interface Sci.* **101** (1984) 511.
[30] R. M. Pashley and J. N. Israelachvili, *Colloids and Surfaces* **2** (1981) 169.
[31] D. J. MacKinnon and J. M. Brannen, *J. Appl. Electrochem.* **7** (1977) 451.
[32] R. Sato, *J. Electrochem. Soc.* **106** (1959) 206.
[33] C. Buelens, PhD thesis, Catholic University of Leuven (1984), pp. 169–83.
[34] P. R. Webb and N. L. Robertson, *J. Electrochem. Soc.* **141** (1994) 669.
[35] C. Buelens, J. P. Celis and J. R. Roos, *J. Appl. Electrochem.* **13** (1983) 541.
[36] B. Dobiáš, 'Coagulation and Flocculation', Surfactant Science Seies 47)Marcel Dekker, New York, 1993).
[37] C. H. Giles and D. Smith, *J. Colloid Interface Sci.* **47** (1974) 755.